Magnetic features of the magmatic intrusion occurred in 2007 eruption at Stromboli Island (Italy)

Rosalba Napoli[1], *Gilda Currenti*[1], *Ciro Del Negro*[1], *Agnese Di Stefano* [1,2], *Filippo Greco*[1] *and Enzo Boschi*[1]

[1] *Istituto Nazionale di Geofisica e Vulcanologia – Sezione di Catania, Italy*

[2] *Dipartimento di Ingegneria Elettrica, Elettronica e dei Sistemi - Università di Catania, Italy*

Dr. Rosalba Napoli: E-mail: napoli@ct.ingv.it, tel. +39 095 7165800; fax +39 095 435801

Abstract

Significant changes in the local magnetic field marked the resumption of the eruptive activity at Stromboli volcano on February 27, 2007. After differential magnetic fields were filtered from the external noise by adaptive filters and from the seasonal thermic noise using temperature data, we highlighted step-like changes of 1-4 nT coincident with the eruptive fissures opening in the upper part of the Sciara del Fuoco. The magnetic variations detected at 2 stations are closely related to the propagation of a shallow NE-SW magmatic intrusion outside the summit craters area . These observations are consistent with those calculated from piezomagnetic models, where stress-induced changes in rock magnetization are produced by the magmatic intrusion. No significant magnetic changes were observed when the first fractures opened along the NE crater rim. Indeed, the stress-induced magnetization caused by this magmatic activity is expected to be too low because of the structural weakness and/or thermal state of the summit area. The continuous long-term decay characterizing the post-eruptive magnetic pattern was related to a time-dependent relaxation process. A Maxwell rheology was assumed and the temporal evolution of the piezomagnetic field was evaluated. This allowed for the estimate of the rheological properties of the medium, in particular an

30 average viscosity ranging between 10^{16} and 10^{17} Pa·s was achieved involving a relaxation
31 time τ of about 38 days.
32
33
34 ***Key words*** – Stromboli Island, magnetic monitoring, piezomagnetic field, stress field
35
36 **1. Introduction**
37
38 The Stromboli volcano represents a natural laboratory with its persistent and regular
39 explosive activity, occasionally replaced by effusive activity and "explosive paroxysm"
40 (Barberi et al., 1993, Barberi et al., 2009), and the high quality geophysical observations
41 gathered by monitoring networks. Since the early nineties the volcano is observed by a
42 ground monitoring system centered on the control of stress and strain releases by use of
43 seismic and deformation networks (Falsaperla et al., 2003; Bonaccorso, 1998). Hitherto, this
44 combination has proved poor successful in detecting magma ascent, tracking intrusion and
45 forecasting the expected sites of lava breakouts in and from the shallow plumbing system.
46 The 2002-2003 eruptive activity, which was accompanied by a tsunami and a paroxysmal
47 vulcanian-type event with strong explosions and lava flows (Bonaccorso et al., 2003), has
48 focused attention on the need to better the knowledge of the volcano internal plumbing system
49 and suggested an improvement of the existing monitoring system. A progressive upgrade of
50 the seismic and deformation networks, that were operating at the onset of the 2002 eruption,
51 and installation of new measurements devices were required. In particular, the systematic
52 observation of the geomagnetic field time changes at Stromboli may be a useful method to
53 gather long-term information about ongoing dynamic processes during times of apparent rest
54 as already proved on volcano worldwide (Zlotnicki and Bof, 1998; Sasai et al., 2002; Del
55 Negro and Currenti, 2003; Del Negro et al., 2004; Napoli et al., 2008). Stromboli is

56 theoretically a favorable site for the observation of volcanomagnetic phenomena. Intense and
57 nearly continuous release of seismic energy by volcanic tremor and explosions, whose
58 sources are concentrated at depths shallower than 200 m beneath the summit craters, seems to
59 be produced by inflation and deflation alternation in the conduits (Chouet et al., 2003). The
60 sequence of pressurization-depressurization, provides favorable conditions to observe and
61 characterize piezomagnetic phenomena caused by stress field changes. Moreover, the
62 presence of a shallow aquifer and large thermal anomalies at its summit (Revil et al, 2004),
63 supports the possibility that the main paroxysmal eruptions of Stromboli can be related to
64 phreatomagmatic processes (Finizola et al., 2003). In this case, it is possible that these
65 eruptions can be preceded by significant thermomagnetic and electromagnetic changes easily
66 detectable by a suitable magnetic array. On the basis of these evidences a small permanent
67 magnetic network, for high resolution measurements of the total field, was installed at
68 Stromboli at the beginning of 2003.

69 The ability of our magnetic network to detect volcanomagnetic effects was proved during the
70 flank eruption started on February 27, 2007. The eruption was characterized by the opening at
71 the northern base of the summit area of a 200 m long NE-SW fissure from which lava coming
72 out rapidly and reached the sea. Successively, the fissure propagated further downslope,
73 varying its strike from NE–SW to NW–SE becoming parallel to the northern rim of the Sciara
74 del Fuoco, a collapsed sector delimited by a horseshoe-shaped scarp (Neri et al., 2008; Neri
75 and Lanzafame 2009). The fractures propagation was accompanied by a sharp increase of the
76 volcanic tremor (Ripepe et al., 2009). The eruptive activity lasted until to the beginning of
77 April 2007 (Barberi et al., 2009).
78 We detected significant changes in the local magnetic field at Stromboli when eruptive
79 fissures propagated outside the summit craters area. Data collected from the permanent
80 magnetic network are analyzed below and the strategy developed to remove variations no

81 related to the volcano activity and enhance signal-to-noise ratios is presented. The magnetic
82 variations were related to stress redistribution due to a dike emplacement and downslope
83 propagation, which took place in a few hours. In the following, the physical mechanisms,
84 which could produce these magnetic field variations, and simple models of the main
85 structures involved with the eruption are proposed. Finally, post-eruptive magnetic variations
86 were related to a viscoelastic relaxation process of a Maxwell rheology undergoing in the
87 volcano edifice.
88
89 **2. The magnetic network**
90 Taking advantage of the experiences gathered at Mt Etna (Del Negro et al., 2002; Del Negro
91 and Currenti, 2003; Del Negro et al., 2004), the Laboratory of Geomagnetism of INGV-CT
92 has designed and has been operating a small permanent magnetic network for high resolution
93 measurement of the total field at the Stromboli Island since 2003. The present network
94 consists of 3 continuously recording stations SPL, SPC and SLN (Fig. 1), spread over the
95 island at elevations ranging between 20 and 500 m a.s.l. (Table 1). The sites were carefully
96 chosen in areas with low magnetic gradient (less than 50 nT/m). The network was designed
97 and set up with inter-station distance less than 2 km, so in case of shallow events this would
98 allow for the direct location of the anomaly source position. Moreover, this layout
99 symmetrical with respect to the central craters should allow to monitoring the geomagnetic
100 field over the whole volcanic edifice.
101 All stations were devised using robust technologic components, which guarantee
102 uninterrupted working under harsh environmental conditions. They were equipped with
103 GSM-90G Overhauser effect magnetic gradiometers (resolution 0.01 nT) consisting of two
104 sensors, oriented vertically above each other at about 50 cm, which simultaneously sample the
105 Earth's magnetic field every 5 seconds. Simultaneously with magnetic signal, atmospheric

106 and ground temperature are acquired at each station. Data are transmitted via mobile phone to
107 the Catania Section where are processed and analyzed in near-real-time. A Global Positioning
108 System (GPS) receiver controls the synchronization of readings. In 2005 one electrical station
109 was also installed at the same site of SLN to acquire self-potential signals. Through joint
110 magnetic and self-potential measurements, effects due to electrokinetic phenomena can be
111 easily distinguished from those due to other sources. A good time correlation between
112 electrical and magnetic signals could indicate the presence of electrokinetic sources. The
113 station is equipped with five Pb-PbCl2 pipe non-polarizing electrodes buried at 0.5 m depth.
114 The measuring dipoles, 50 and 100 m long, are orthogonally oriented along a NS and EW
115 direction. By this dipole arrangement, noise from electrode instability, rainfall and nearby
116 sources can be reduced.
117
118 **3. Magnetic observations from 2005 to 2007**
119 Over the last decades volcanomagnetic monitoring has been playing an increasing role for
120 improving the knowledge of the geophysical processes preceding and accompanying volcanic
121 unrest (Zlotnicki and Bof, 1998; Del Negro et al., 2004; Napoli et al., 2008). Volcano
122 monitoring is concerned with detection of local magnetic field changes attributable to the
123 dynamics of the volcano's plumbing system and removal of the geomagnetic field variations
124 with no geophysical significance. The rapid changes associated with volcanomagnetic events
125 are usually very small, within 1~10 nT, and must be detected in the presence of considerable
126 noise produced by natural geomagnetic fluctuations of external origin, which make the
127 detection of volcanic source effects more difficult and may lead to misinterpret data. In
128 general, the classical differential technique, based on simultaneous simple differences among
129 the magnetic field amplitudes recorded at several points on a volcano, is the most frequently
130 used and reliable method to remove them. In Fig. 2 daily averages of total intensity variations

131 from 2005 to 2007 observed at SLN, SPC and SPL stations, relative to the reference station
132 CSR installed further south (about 100 km) on the Nebrodi Mountains, Sicily, are shown. A
133 slow and continuous decrease in the magnetic field total intensity was observed at SLN,
134 which is located in the eastern side of the volcano and it is the station closest to summit area.
135 SPC and SPL stations, located respectively on the western and southern flanks of Stromboli,
136 did not show any long-term trends. The total intensity decreased by about 10 nT within 2
137 years at SLN station. It is possible to suppose that this long-term trend could be related to the
138 global activity of the volcano. Stromboli, indeed, is an open-conduit volcano characterized by
139 continuous refilling, mixing and magma eruption (Metrich et al., 2010). Generally, the
140 magma upraise mechanism involves low energy and not always clear geophysical signals are
141 observed, however, this uniform eruptive regime may generate quasi continuous magnetic
142 activity. Much of the volcanic energy, indeed, is dissipate by the very active hydrothermal
143 system developed in the volcanic edifice of Stromboli (Finizola et al., 2003) and the
144 circulation of magmatic gases, heat and meteoric water could promote thermomagnetic and
145 electrokinetic effects. The time-scale of the magnetic change is compatible with both effects
146 or a combination of them. Moreover, considering the interpretative section of fluid circulation
147 of Stromboli obtained by Finizola et al. (2003; 2006), SLN is the only station of the network
148 located above the self-sealing zone of the hydrothermal system very near to the N 40 regional
149 fault, a structure that significantly contribute to the heat supply of the hydrothermal system.
150 Therefore, even if the long trend is observed at only one station we favor a more
151 straightforward explanation in terms of thermomagnetic effects. On this linear trend, an
152 annual periodic geomagnetic component is superimposed, as well as in the differences of
153 other stations. It is evident that, even if differencing technique is properly employed,
154 geomagnetic fluctuations have clearly been observed in the magnetic reduced signals
155 regardless of the state of the volcanic activity.

156

157 *3.1 Data processing*

158 Main sources for natural geomagnetic fluctuations are electric current systems of ionospheric
159 and magnetospheric origin related to the solar activity. Time variations of the external current
160 systems produce time-varying magnetic fields that induce electric currents inside the earth by
161 electromagnetic induction. These induced currents in turn produce time-varying magnetic
162 fields. At Stromboli the electrical conductivity of the rocks changes over short distances
163 (Finizola et al. 2006), consequently time changes can vary correspondingly. In addition,
164 variable induced magnetization, due to large susceptibility contrasts (Speranza et al., 2004),
165 could locally modify a magnetic disturbance field by an amount up to 5 nT (Davis et al.,
166 1979, Del Negro et al., 2004). These effects are highlighted at SPC station, where in
167 correspondence of strong external activity high geomagnetic components clearly appear in the
168 differences (Fig 2).

169 To reduce the changes in the difference fields due to contrasting responses at magnetometer
170 sites, we applied predictive filtering techniques, with the filters giving the relative responses
171 between the sites. In particular, an adaptive type approach was implemented (Del Negro et al.
172 2004). taking in consideration that total field differences depend on the direction of the
173 disturbing field. When the local total field is added to external field and to locally induced
174 magnetization, different increments appear at each site because of the difference in the
175 orientation of the local total fields. To remove these variations it needs information in the
176 direction of the difference vector. We used the three components of the vector magnetometer
177 of L'Aquila Geomagnetic Observatory (Fig. 3), which is the vector magnetometer closest to
178 the reference station. Even if L'Aquila Geomagnetic Observatory is about 400 kilometers
179 away from Stromboli, signals correlate well. The correlation coefficients, calculated between
180 total magnetic field data at Stromboli stations and L'Aquila observatory from 2005 to 2007,

181 are about 0.90. In this case, the three component fields of the vector magnetometer at
182 L'Aquila and the total field at CSR reference station (of Stromboli array) are used to reduce
183 the data at the two stations (SLN and SPC).
184 To emphasize magnetic fluctuations a simple linear trend was removed from all the signals.
185 The residual components, shown in Figure 3, reveal that the high frequency components are
186 effectively removed at all stations. On the other hand the annual periodic geomagnetic
187 components are highlighted in all the magnetic sequencesThe amplitude of these annual
188 changes is about 4 nT at SPL and SLN while it is lesser than 2 nT at SPC.
189 Cross-correlation analysis in the time domain between geomagnetic signals and temperature
190 show that these cyclic changes are well correlated with seasonal temperature variations. The
191 correlation indexes for the different sites range between 0.5 and 0.8 (Table 2). It is worth
192 noting that the strongest correlation with temperature is observed at SPL that is located in the
193 southern side of the island where there is the maximum insulation.
194 Annual variations can occur for two main causes: (i) a thermal drift of magnetometers, or (ii)
195 slow thermomagnetic processes in shallow rocks. We exclude the first reason because
196 laboratory test (Leotta, 2007) carried out in the temperature operating range of Overhauser
197 effect magnetometers, that is from -40°C to +60°C, reveal a thermal sensitivity of about 0.025
198 nT/°C. Moreover, the temperature range on Stromboli is from +5°C to +40°C. On the other
199 hand, recent and more accurate studies claim that annual periodic variations in the
200 geomagnetic total intensity could be caused by seasonal changes in the heterogeneous
201 magnetization of near-surface rocks due to a diffusion of atmospheric temperature changes
202 into the ground. Using the method proposed by Utada et al. (2000), the features of annual
203 variations (ΔFT) can be quantitatively explained by analyzing field data and examining the
204 magnetic properties of rock samples from Stromboli Island. By applying this method, the
205 annual variations can be removed with a simple first order linear filter (Del Negro and

206 Currenti, 2003) Figure 4 shows that the simple linear filtering is effective enough, indeed, the
207 periodical fluctuations are completely removed at all stations and the changes on February 27
208 are the only significant ones during the observed period.
209
210 **4. Magnetic Interpretation**
211 We didn't detect remarkable variations before February 27, while a step-like variation at SPC
212 and SLN stations accompanied the opening of the eruptive fissures in the upper part of the
213 Sciara del Fuoco. The total magnetic field undergoes an irreversible change (Fig. 4).
214 Continuous self-potential measurements recorded at SLN station show annual fluctuations
215 likely correlated with ground temperature variations but did not reveal significant variations at
216 the time of the eruption onset (Fig. 5). Since no remarkable electric field variations were
217 observed, electrokinetic effects can be disregarded (Currenti et al., 2007). Comparison of the
218 reduced data with the volcanic events occurring here showed the close temporal
219 correspondence between the magnetic variations and the quick propagation of the eruptive
220 fissure from the summit area to the rim of the Sciara del Fuoco. A continuous long-term
221 decay was also observed after the end of the eruption. Since the beginning of April 2007 the
222 daily variations of total magnetic intensity with respect to CSR station gradually decreased
223 within 5 months (Fig. 4). Therefore, the geophysical source which could produce these
224 magnetic field variations was searched.
225 The magnetic data gathered at SPC and SLN stations are not dense enough to uniquely
226 identify the physical process that generated the observed anomalies, however, a preliminary
227 interpretation is possible by taking into account other available geophysical data.
228 In the morning of February 27, since 9:13 GMT, the seismic network operated by INGV
229 recorded an abnormal increase of the number of seismic events related to small landslides on
230 the Sciara del Fuoco (Barberi et al., 2009). The infrasonic array showed that explosive and

231 degassing activity ceased at 10:32 GMT, a couple of hours before the opening of the effusive
232 fractures. The end of the explosive activity coincided with an intense phase of high-frequency
233 tremor reaching the maximum amplitude almost 8 h after the explosive activity at the summit
234 craters had stopped (Ripepe et al., 2009). An initial phase of large ground inflation was
235 followed at about 11:20 GMT by a gradual inversion of the deformation field (Marchetti et al
236 2009). However, the images of the video monitoring system of the INGV showed the first
237 fissure propagating within the NE crater at 12:00 GMT (Barberi et al., 2009; Calvari et al.,
238 2010), while thermal cameras of University of Firenze and INGV observed the onset of lava
239 effusion at about 12:49 GMT at the base of the NE crater (Ripepe et al., 2009). The fissure
240 reached a minimum elevation at about 400 m asl, where a new vent opened at 18:26 GMT.
241 The opening of this new vent was accompanied by a sharp increase of seismic tremor, a small
242 inflation/deflation cycle and a strong infrasonic signal (Barberi et al 2009; Ripepe et al 2009).
243 In Figure 6 the 10-minute means of total intensity from February 24 to March 2 are shown.
244 The removal of external components by adaptive filtering allows to better estimate the
245 volcanomagnetic changes. Until 13:00 GMT no significant changes were observed at both
246 magnetic stations, soon after, the total intensity sharply increased with amplitudes of about 1
247 nT at SPC and 4 nT at SLN. The variation at the two magnetic sites occurred about ten
248 minutes after the eruption onset as revealed by thermal cameras. The simultaneity and
249 proximity in space and time of the observed anomaly argue in favor of a piezomagnetic effect
250 as the primary physical mechanism driving these transient changes. The variation could have
251 resulted from stress redistribution in time correspondence with the migration of the effusive
252 vents and the outpouring lava flows in the upper part of the depression of the Sciara del
253 Fuoco. To infer the source and provide information on the on-going crustal movement
254 associated with magma migration, we developed a mechanical model based on the opening
255 and the propagation pattern of the NE-SW eruptive fissure on the volcanic edifice. We

256 presumed that magma pressurized within the central conduit of Stromboli volcano and
257 laterally propagated along a NE-SW fracture from the base of the summit area up to the
258 northern rim of Sciara del Fuoco. The interpretation of magnetic data was performed taking
259 into account the 3D reconstruction of the propagation paths of the dykes feeding eruption
260 (Neri et al., 2008; Neri and Lanzafame 2009) and other geophysical data. The ground
261 deformation that accompanied the lava effusion suggests a dyke-shaped structure striking
262 40°N, which is consistent with the position of the effusive vent opened in the Sciara del
263 Fuoco (Marchetti et al., 2009). Thermal-camera based observations (Calvari et al., 2010)
264 allowed to assess the direction of two effusive fractures development. The first opened at the
265 northeastern base of the NE crater and quickly propagating NE, successively the feeder dike
266 propagated downslope along the NW-SE detachment surface beneath the sliding portion of
267 the Sciara del Fuoco (Calvari et al., 2010). This is consistent with fractures pattern detected at
268 the ground surface by Neri and Lanzafame (2009).
269 The magnetic changes could have generated from stress redistribution due to dike
270 emplacement and downslope propagation, which took place in a few hours. We employed a
271 piezomagnetic elastic model, based on the analytical solution in Utsugi et al. (2000), to
272 estimate the co-eruptive magnetic field change at the earth's surface. On the basis of thermal
273 observations, we considered two tensile fractures that are the direct effect of the stress
274 produced by dike intruding and traveling near-horizontally at shallow depth. The length
275 (along-strike dimension) and strike of the fracture segments are determined by the field
276 mapping data (Neri and Lanzafame, 2009) and are listed in Table 3 together with estimates of
277 rock magneto-elastic properties. The rock magnetization was calculated from surface samples
278 near the various magnetometer sites (Speranza et al, 2004). The Lame's constant were set up
279 to $\lambda = \mu = 30$ GPa giving a Poisson's ratio of 0.25, a reasonable approximation to the values
280 estimated in basaltic rocks. Fig. 7 shows the calculated anomaly from the piezomagnetic

281 model. The computed values from this model are in good agreement with the observed local
282 magnetic field data.
283 It is worth noting that the magnetic field, after the step-like variation remained constant,
284 supporting the idea that the field is maintained by the stress buildup accompanying the
285 eruption.
286 At the beginning of April 2007, when the eruptive activity ended, a decay in the magnetic
287 field is observed. Significant time-dependent piezomagnetic changes can be expected as a
288 result of viscoelastic relaxation processes. The influence of post-eruption viscoelastic
289 relaxation of the crust on the piezomagnetic field can play a role in long-term magnetic
290 observations. We investigated the piezomagnetic response of dislocation sources embedded in
291 viscoelastic medium to interpret these time-dependent magnetic variations. The magnetic
292 changes show an exponential decrease, which is consistent with computed time-dependent
293 changes in a homogeneous medium with a Maxwell rheology (Currenti et al., 2008). The
294 viscoelastic solution at the beginning of the decay is identical to the elastic one, which was
295 used to estimate the dislocation parameters at the eruption onset. Starting from these model
296 parameters, we evaluated the temporal evolution of the piezomagnetic field (Fig. 8). The
297 temporal decay of the magnetic variations allows for the estimate of the rheological properties
298 of the medium. The viscoelastic model based on the analytical solution in Currenti et al., 2008
299 matches the long-term magnetic variations using a relaxation time $\tau = \frac{\eta}{\mu}$ of about 38 days,
300 where η and μ are the viscosity and the rigidity of the surrounding rocks, respectively. For an
301 average rigidity ranging between 3 and 30 GPa, the estimated viscosity (η) varies from 10^{16} to
302 10^{17} Pa·s.
303
304
305

5. Discussion

After the end of the 2002–2003 eruption, Stromboli volcanic activity returned to typically persistent but moderate explosive activity until February 27, 2007 when a new eruption started. The eruption onset was preceded by significant geophysical parameter changes. In particular seismic activity and ground deformation showed an abrupt increase, suggesting that magma arose within the shallow feeding conduit (Barberi et al., 2009; Marchetti et al., 2009) and then lateral propagated along the main NE-SW tectonic trend that cuts the volcano (Neri and Lanzafame, 2009). Until 13:00 GMT, no evident changes were detected at all magnetic stations. Volcanomagnetic signals appear only at 13:00 GMT when eruptive fissures is opening along the northern flank of the NE crater rim from 11 minutes and when deflation phenomenon begin since 1 hours and 40 minutes. The lack of an observable piezomagnetic effect correlated with the initial phase of the intrusive process can be interpreted as evidence that, by virtue of its structural weakness, the summit area of the volcano can support only limited stresses, insufficient to permit the development of a significant piezomagnetic anomaly. Neri and Lanzafame (2009) supposed the new eruptive fractures probably used preexisting detachment surfaces. Similarly to 2002-03 eruption the fracture systems feeding this eruption started with a dike intrusion from the summit crater area toward NE. This appears to be the recurring eruptive dynamics, reflecting a structural weakness of the complex region surrounding the summit craters (Neri and Lanzafame, 2009). However, this is not the only possible explanation for any magnetic changes. Considering that Stromboli is an open conduit volcano with persistent explosive activity, we can assume the summit area is constantly penetrated by fresh magma, very high-temperature liquids and gases originating from magma itself. The magma and hot fluids are likely to have penetrated outwards through cracks and pores to efficiently raise the temperature of the surrounding rocks. The injection of magma and hot fluids can lead to extensive conductive and convective thermal exchanges,

331 which can strongly lower the initial magnetization of nearby large volumes (Yukutake et al.,
332 1990, Del Negro and Napoli, 2004). Piezomagnetic changes are approximately proportional to
333 the applied stress and the initial magnetization, therefore no piezomagnetic effects would be
334 seen in this area, whatever the internal stresses are.
335 The intrusive dike estimated by magnetic data is very shallow, about 300-350 m asl, in
336 agreement with the deformation source from Marchetti et al. (2009). However, the extension
337 and geometry of the magnetic and deformation models are quite different. Magnetic data
338 interpretation, indeed, indicated the response to a tensile mechanism with an intrusion
339 crossing the summit area of Stromboli producing two fractures, with a NE-SW and NW-SE
340 direction respectively, which developed in few hours in the Sciara del Fuoco. This is
341 consistent both with thermal based observations (Calvari et al., 2010) and fractures pattern
342 detected at the ground surface by Neri and Lanzafame (2009).
343 At about 16:30 GMT on 27 February, in correspondence with the increasing of the volcanic
344 tremor, magnetic changes show a rate increase supporting the hypothesis that the magma
345 injection was still ongoing (Fig. 6). Indeed, the downward propagation of the magmatic dike
346 produced the opening of the new eruptive vent at 400 m asl at 18:26 GMT. After 20:00 GMT
347 no further magnetic variations were observed, and geomagnetic total intensity at all stations
348 turned almost flat at a new level. While significant magnetic changes were associated to the
349 opening and the propagation in the upper part of the Sciara del Fuoco of the NE-SW
350 magmatic intrusion on February 27, the eruptive fractures opened on March 9 in the central
351 portion of the Sciara del Fuoco did not produce stress-induced magnetic changes, probably
352 because of the highly fractured nature of this area.
353 Post-eruptive magnetic changes related to stress relaxation process within the medium were
354 also observed. Assuming a Maxwell rheology, the proposed piezomagnetic model was able to
355 fit the temporal variations in the local magnetic field observed during and after the magmatic

intrusions in the Sciara del Fuoco. The time scale of the magnetic variations involves a viscosity (η) that varies from10^{16} to 10^{17} Pa·s. The viscosity η values obtained are lower than most of the viscosity estimates for continental lower crust (e.g.~10^{19}–10^{20} Pa s; Hearn et al., 2002; Hearn, 2003; Sheu and Shieh, 2004). On the other hand, the low viscosity values can be the result of the high temperature field generated by the continuous refilling, mixing and magma eruption. Moreover, the estimated values at Stromboli are in agreement with those in Newman et al (2001) where an average viscosity values of about 10^{16} Pa s was obtained at Long Valley Caldera through the analysis of long-term deformation observed during period of unrest. Our study shows up that magnetic observations can also allow gaining insights into time-dependent geophysical changes and into the rheology of medium.

Therefore, replacing elastic half-space models with more realistic approximations of viscoelastic rheologies could improve the interpretation of geophysical changes associated with volcano activity (Currenti et al., 2008). In particular, the relaxation time τ inferred by viscoelastic models provides information about the time decay of the anomaly observed that could play an important role for the evaluation of a volcanic crisis and the related hazard alert level. It is worth noting that a viscoelastic half-space is too crude an approximation to properly describe earth's crust and the relation between viscosity and depth and material has to be considered. This may be a rather laborious work, but could make a breakthrough to further tectonomagnetic studies.

6. Conclusions

The magnetic network at Stromboli Island is aimed to improve the geophysical knowledge on the dynamics of the shallow plumbing system of the volcano by the study of transients associated with the modifications within the volcanic edifice of the stress field or of the thermodynamic state. Although the network is composed of only three Overhauser effect

magnetometers continuously recording the intensity of the Earth magnetic field, crucial information about volcanic processes within the shallow part of the edifice was inferred.

Long and short-term variations were clearly observed since 2005 at SLN. The long-term changes show an abrupt increase of the variation rate from March to July 2006. This period spans: (i) the unusual seismic activity occurred in the period April-May 2006 (D'Auria et al., 2006), (ii) the increase in the amplitude of the seismic tremor observed in the period July–August 2006 (Barberi et al., 2009), and (iii) the inflationary trend revealed by tiltmeters during the summer 2006 (Bonaccorso et al., 2009). Therefore, magnetic data together with other volcanological and geophysical evidences provided insights of the anomalous state of the volcano. The long-term magnetic change cannot be interpreted in term of piezomagnetic effect, which should be in conflict with the variations observed in the other stations. Thermomagnetic effect could be the main mechanism responsible of this variation due to the proximity of the SLN station to the hydrothermal source. On the basis of only one measurement point, it is not possible to constrain the source parameters. Local magnetic surveys at SLN as well as installation of a new magnetic station in the summit area could provide new constraints to identify the position and geometry of the source and to better clarify the origin of this long-term trend.

Remarkable short-time changes accompanied the eruptive fissure openings during the 2007 Stromboli eruption. Magnetic changes are not synchronous with the beginning of the eruption at 12:49 GMT, when eruptive fissures opened along the northern flank of the NE crater rim. In this area structural weakness and thermal conditions provide unfavorable environment to observe and characterize piezomagnetic phenomena caused by stress field changes. The piezomagnetic changes were simultaneously observed at both magnetic stations about 10 minutes after the onset of eruption, when eruptive fissures propagated outside the summit area. They clearly indicated modifications of the stress field within the volcanic edifice due to

406 gas overpressure or magma injection or a combination of both (Metrich et al., 2010). A simple
407 magnetic model allowed us to infer the position and the geometry of the sources, which could
408 explain the total intensity change. In this case magnetic observations provided valuable
409 information on what happened at a rather shallow depth beneath the volcano.
410
411
412 **Acknowledgements**
413 We are indebted to all personal of Division of Gravity and Magnetism of INGV-Sezione di
414 Catania who ensure the regular working of the permanent magnetic network at Stromboli
415 Island. The authors are grateful to the Italian civil protection for support during setting of the
416 network. We are grateful to the Associated Editor Maurizio Ripepe, Takeshi Hashimoto and
417 an anonymous reviewer for their helpful comments.
418
419
420 **References**
421 Barberi, F., Rosi, M., Sodi, A., 1993. Volcanic hazard assessment at Stromboli based on
422 review of historical data. Acta Vulcanol. 3, 173–187.
423 Barberi, F., Civetta, L., Rosi, M., Scandone, R., (2009). Chronology of the 2007 eruption of
424 Stromboli and the activity of the Scientific Synthesis Group. Journal of Volcanology and
425 Geothermal Research 182, 123–130
426 Bonaccorso A (1998) Evidence of a dyke-sheet intrusion at Stromboli volcano inferred
427 through continuous tilt. Geophys Res Lett 25 (22), 4225.
428 Bonaccorso A, Calvari S, Garf ì G, Lodato L, Patane` D. (2003) Dynamics of the December
429 2002 flank failure and tsunami at Stromboli volcano inferred by volcanological and
430 geophysical observations. Geophys Res Lett 30,18, 1941, doi:10.1029/2003GL017702.
431 Bonaccorso A., Bonforte A., Gambino S., Mattia M., Guglielmino F., Puglisi G., Boschi E.
432 (2009) Insight on recent Stromboli eruption inferred from terrestrial and satellite ground
433 deformation measurements, J. Volc. Geoth. Res., doi:10.1016/j.jvolgeores.2009.01.007.

434 Calvari S., Lodato L., Steffke A., Cristaldi A., Harris A. J. L., Spampinato L., Boschi E.
435 (2010) The 2007 Stromboli eruption: Event chronology and effusion rates using thermal
436 infrared data. J of Geophys Res, 115, doi:10.1029/2009JB006478.
437 Chouet B, Dawson P, Ohminato T, Martini M, Saccorotti G, Giudicepietro F, De Luca G,
438 Milana G, Scarpa R (2003) Source mechanisms of explosions at Stromboli Volcano, Italy,
439 determined from moment-tensor inversions of very-long-period data. J of Geophys Res,
440 108, B1, 2019, doi:10.1029/2002JB001919.
441 Currenti G, C Del Negro, D Giudice, R Napoli, A Sicali (2007) Isola di Stromboli: rapporto
442 sulle osservazioni magnetiche aggiornamento del 9 marzo 2007. INGV Rep.
443 RPTGM20070309, Ist. Naz. Di Geofis. e Vulcanol., Rome.
444 Currenti G, Piombo A, Del Negro C, Dragoni M (2008) Piezomagnetic fields due to an
445 inclined rectangular fault in a viscoelastic half-space: an application to the 2002–2003 Etna
446 eruption. Geophys J Int 175: 901–912
447 Davis PM, Stacey FD, Zablocki CJ, Olson JV (1979) Improved signal discrimination in
448 tectonomagnetism: discovery of a volcanomagnetic effect at Kilauea, Hawaii. Phys Earth
449 Planet Inter 19: 331– 336.
450 D'Auria, L., Giudicepietro, F., Martini, M., Orazi, M., 2006. The April-May 2006
451 volcanotectonic events at Stromboli volcano (Southern Italy) and their relation with the
452 magmatic system. http://hdl.handle.net/2122/1506.
453 Del Negro C, Napoli R, Sicali A (2002) Automated System for Magnetic Monitoring of
454 Active Volcanoes. Bull Volcanol 64: 94-99.
455 Del Negro C, Currenti G (2003) Volcanomagnetic signals associated with the 2001 flank
456 eruption of Mt. Etna (Italy). Geophys Res Lett 30(7), 1357, doi:10.1029/2002GL015481.
457 Del Negro C, Napoli R (2004) Magnetic Field Monitoring at Mt. Etna During the Last 20
458 Years. In: "Etna Volcano Laboratory" Bonaccorso, Calvari, Coltelli, Del Negro, Falsaperla
459 (Eds), AGU (Geophysical monograph series; 143), 241-262, ISBN 0-87590-408-4.
460 Del Negro C, Currenti G, Napoli R, Vicari A (2004) Volcanomagnetic changes
461 accompanying the onset of the 2002–2003 eruption of Mt. Etna (Italy). Earth and Planetary
462 Science Letters 229: 1– 14
463 Falsaperla S, Alparone S, Spampinato S (2003) Seismic features of the June 1999 tectonic
464 swarm in the Stromboli volcano region, Italy. J Volcanol Geotherm Res 125: 121-136.
465 Finizola A, Sortino F, Lenat JF, Aubert M, Ripepe M,Valenza M (2003) The summit
466 hydrothermal system of Stromboli. New insights from self-potential, temperature, CO2 and

467 fumarolic fluid measurements, with structural and monitoring implications. Bull Volcanol
468 65: 486 – 504.
469 Finizola A, Revil A, Rizzo E, Piscitelli S, Ricci T, Morin J, Angeletti B, Mocochain L,
470 Sortino F (2006) Hydrogeological insights at Stromboli volcano (Italy) from geoelectrical,
471 temperature, and CO2 soil degassing investigations. Geophys Res Lett 33, L17304,
472 doi:10.1029/2006GL026842.
473 Leotta MG (2007) Indagine sugli effetti della temperature su magnetometri ad effetto
474 Overhauser. Thesis of Degree, University of Catania.
475 Marchetti E., Genco R., Ripepe R. (2009) Ground deformation and seismicity related to the
476 propagation and drainage of the dyke feeding system during the 2007 effusive eruption at
477 Stromboli volcano (Italy), J. Volc. Geoth. Res., 182, 155–161,
478 doi:10.1016/j.jvolgeores.2008.11.016.
479 Metrich N., Bertagnini A., Di Muro A. (2010) Conditions of Magma Storage, Degassing and
480 Ascent at Stromboli: New Insights into the Volcano Plumbing System with Inferences on
481 the Eruptive Dynamics, J. of Petrology, 51, 3, 603-626, doi:10.1093/petrology/egp083
482 Napoli R, Currenti G, Del Negro C, Greco F, Scandura D (2008) Volcanomagnetic evidence
483 of the magmatic intrusion on 13th May 2008 Etna eruption. Geophys Res Lett 35, L22301,
484 doi:10.1029/2008GL035350,.
485 Neri M., Lanzafame G. (2009), Structural features of the 2007 Stromboli eruption, J. Volc.
486 Geoth. Res., 182, 137–144, doi:10.1016/j.jvolgeores. 2008.07.021.
487 Neri M, Lanzafame G, Acocella V (2008) Dyke emplacement and related hazard in volcanoes
488 with sector collapse: the 2007 Stromboli (Italy) eruption. J of the Geol Soc 165: 883-886.
489 Revil A, Finizola A, Sortino F, Ripepe M (2004) Geophysical investigation at Stromboli
490 volcano, Italy: implications for ground water flow and paroxysmal activity. Geophys J Int
491 157: 426 - 440.
492 Ripepe, M., Delle Donne D., Lacanna G., Marchetti E., Ulivieri G., (2009) The onset of the
493 2007 Stromboli effusive eruption recorded by an integrated geophysical network, J. Volc.
494 Geoth. Res., 182, 131–136, 1129 doi:10.1016/j.jvolgeores.2009.02.011.
495 Sasai Y, Uyeshima M, Zlotnicki J, Utada H, Kagiyama T, Hashimoto T, Takahashi Y (2002)
496 Magnetic and electric field observations during the 2000 activity of Miyake-jima volcano,
497 Central Japan Earth and Planetary Science Letters 203: 769-777
498 Speranza F, Pompilio M, Cagnotti L (2004) Paleomagnetism of spatter lavas from Stromboli
499 volcano (Aeolian Islands, Italy): Implications for the age of paroxysmal eruptions. Geophys
500 Res Lett 31, L02607, doi:10.1029/2003GL018944

501 Utada H, Neki M, Kagiyama T (2000) A study of annual variations in geomagnetic total
502 intensity with special attention to detecting volcanomagnetic signals. Earth Planets Space,
503 52: 91-103.
504 Utsugi M, Nishida Y, Sasai Y (2000) Piezomagnetic potentials due to an inclined rectangular
505 fault in a semi-infinite medium. Geophys J Int 140: 479-492.
506 Yukutake T, Utada H, Yoshino T, Watanabe H, Hamano Y, Sasai Y, Kimoto E, Otani K,
507 Shimomura T (1990) Changes in the geomagnetic total intensity observed before the
508 eruption of Oshima Volcano in 1986, *J. Geomagn. Geoelectr*., 42, 277-290.
509 Zlotnicki J, Bof M (1998) Volcanomagnetic signals associated with the quasi-continuous
510 activity of the andesitic Merapi volcano, Indonesia: 1990-1995. Phys Earth Planet Int 105:
511 119-130.

Table

Station	Location	Latitude	Longitude	Altitude	Acquisition	Transmission
SPL	Punta Lena	518407	4291656	25 m	5 s	GSM
SPC	Punta dei Corvi	516983	4294184	160 m	5 s	GSM
SLN	Liscione	519419	4294516	500 m	5 s	GSM

Tab. 1 - Magnetic stations of the permanent network of Stromboli

Geomagnetic data	Raw data	Filtered data
SLN Up-CSR	0.061	0.46
SLN Low-CSR	0.041	0.50
SPC Up-CSR	0.037	0.78
SPC Low-CSR	0.089	0.80
SPL Up-CSR	0.670	0.86
SPL Low-CSR	0.705	0.86

Tab. 2 - The correlation indexes between geomagnetic signals and temperature before and after removal of the external effects by adaptive filter

Fault	X center (km)	Y center (km)	Depth (m)	Length (km)	Width (km)	Strike	Dip	Dislocation (m)
Tensile	4294.3	518.57	350	0.23	0.7	30°	90°	1.5
Tensile	4294.5	518.56	300	0.1	0.6	-20°	90°	2

Tab. 3 - Summary of fault parameters used in the piezomagnetic model. Magnetization 6 A/m, Inclination 54.7°, Declination 2.22°, stress sensitivity 0.0001 bar^{-1}, and rigidity 30 GPa

Figure

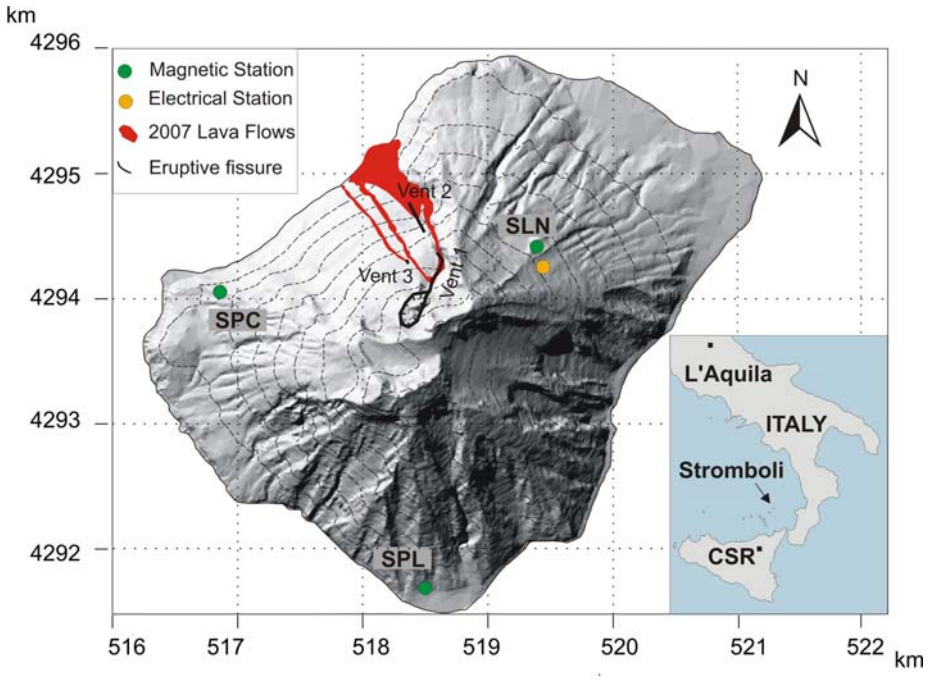

Figure 1 – Schematic map of the 2007 eruptive fractures at Stromboli Island. Locations of magnetic and electrical stations are shown as well. Inset shows the position of the CSR reference station and L'Aquila geomagnetic observatory.

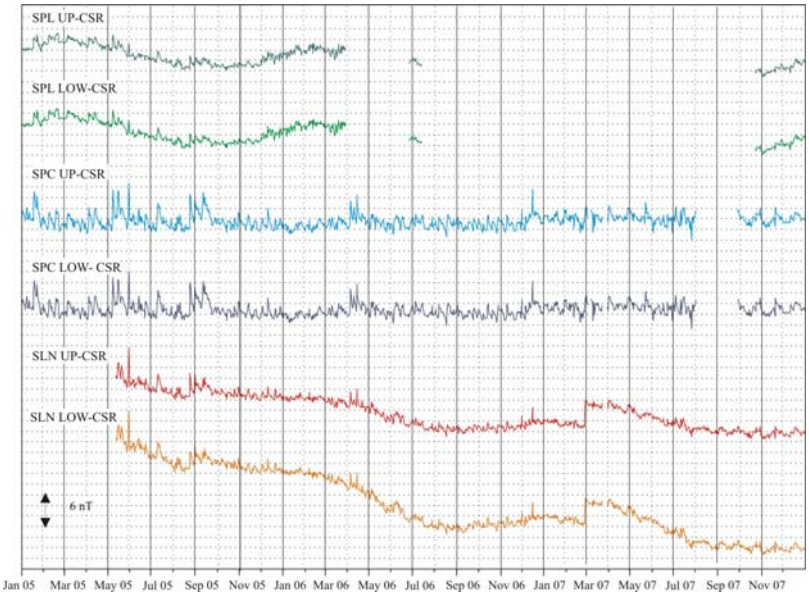

Figure 2 – Daily mean differences of total magnetic intensity with respect to CSR station from January 2005 to December 2007.

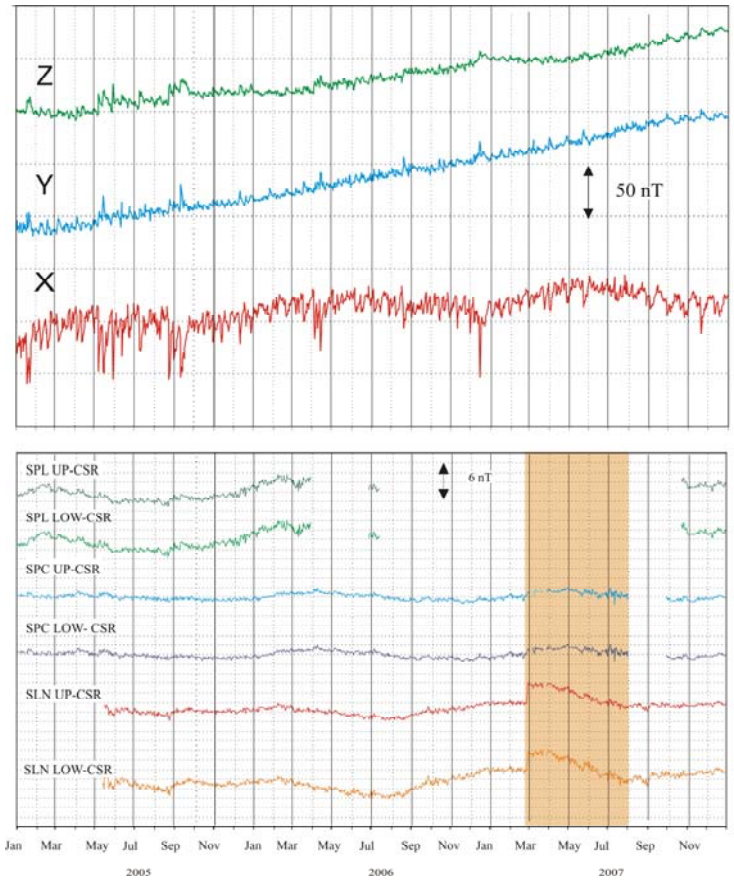

Figure 3 – Three component fields of the vector magnetometer at L'Aquila used as inputs to the adaptive filter (top). Residual components of the daily means of total magnetic intensity after removing external effects by filter (bottom).

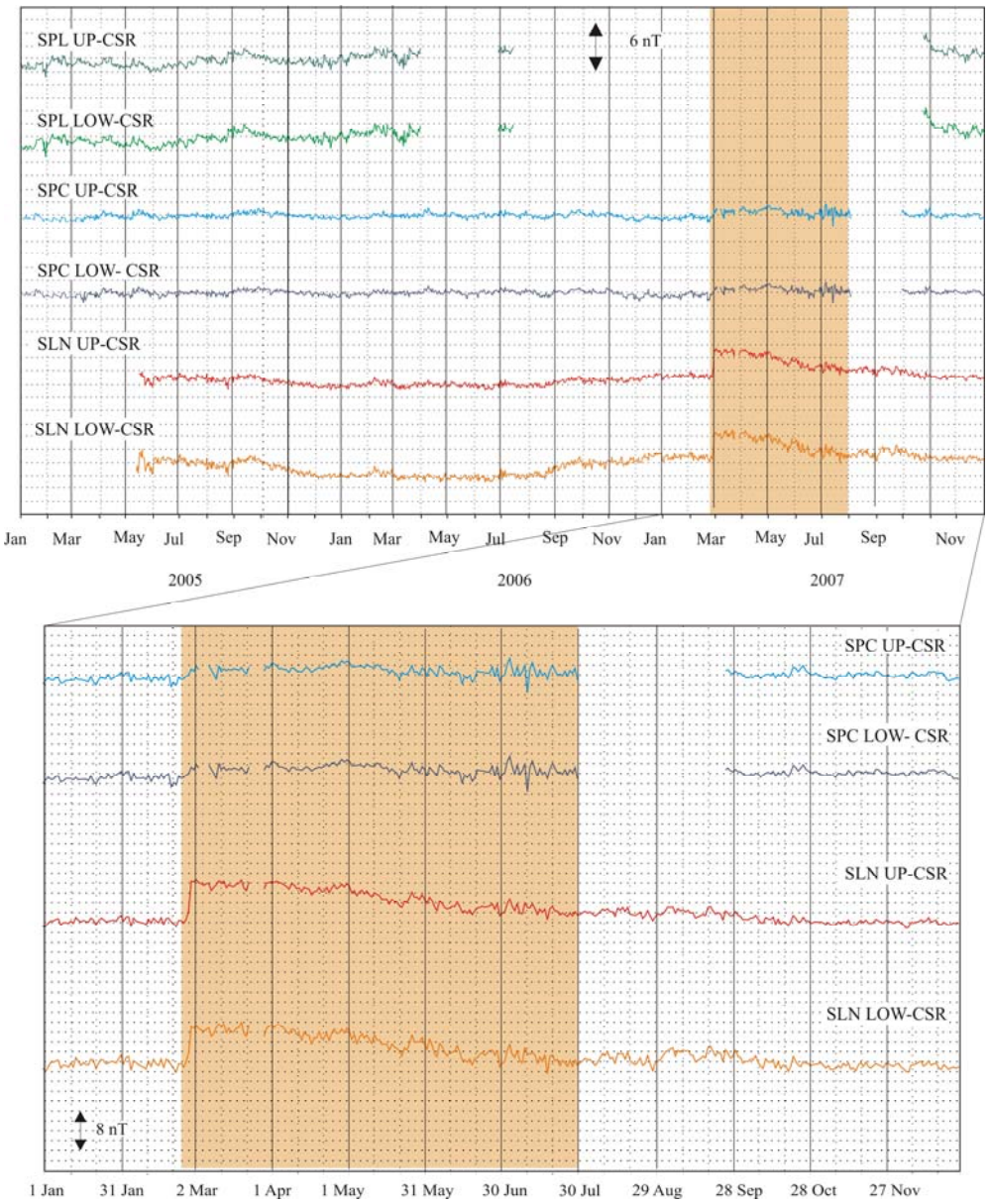

554
555

556 **Figure 4 –** Residual components of the daily means of total magnetic intensity after removing (top)
557 periodic fluctuations by one linear filter. Data from January to December 2007 are shown up (bottom).

558

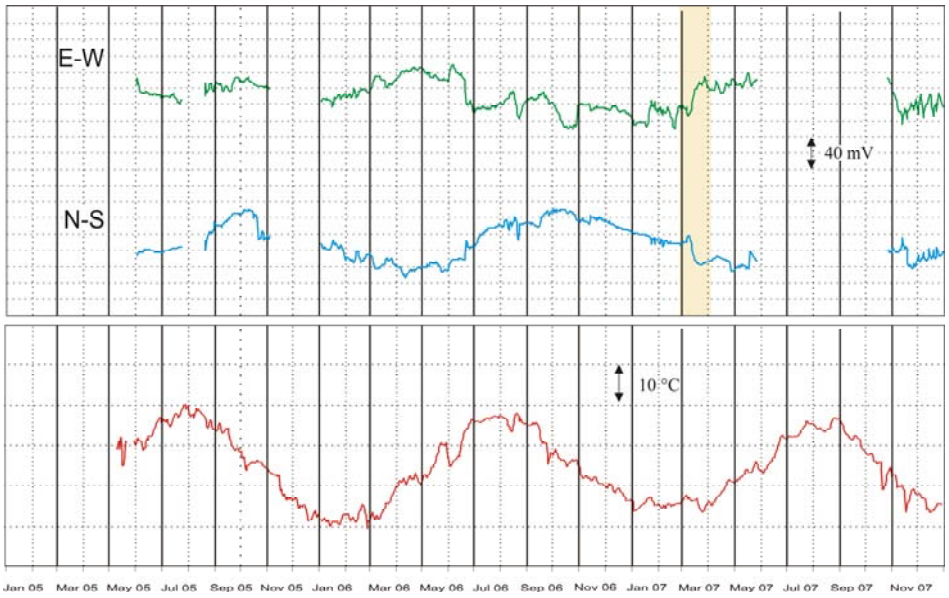

559
560
561

562 **Figure 5** – Daily mean of Self Potential measurements of EW and NS components (top) and of
563 ground temperature(bottom) observed at SLN station from 2005 to 2007.

564
565
566
567
568
569
570
571
572
573

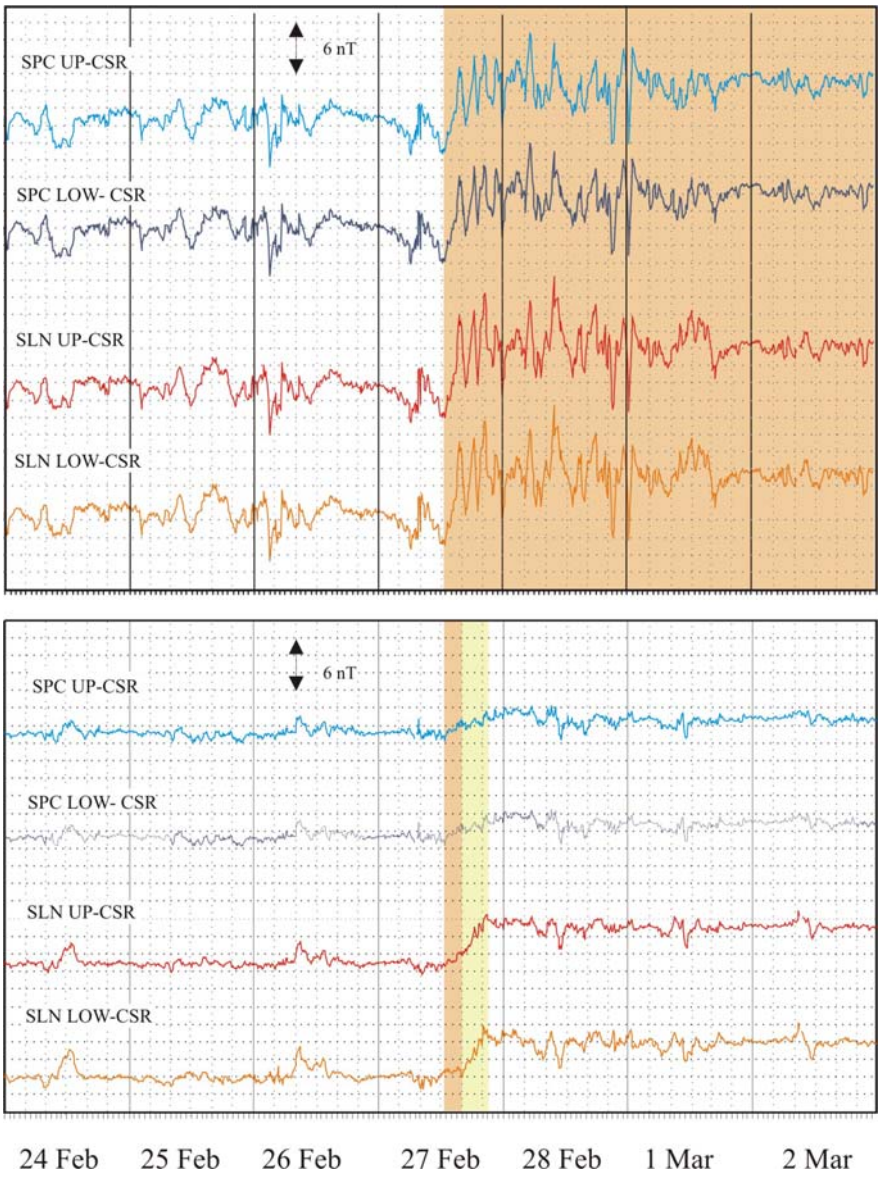

574

575

576 **Figure 6 –** 10-minute means of total magnetic intensity from February 24 to March 2, 2007 (top).
577 Residual components of the 10-minute means of total magnetic intensity after removing external
578 effects by adaptive filter (bottom). Piezomagnetic changes started at about 13:00 GMT are
579 highlighted.

580

581

582

583

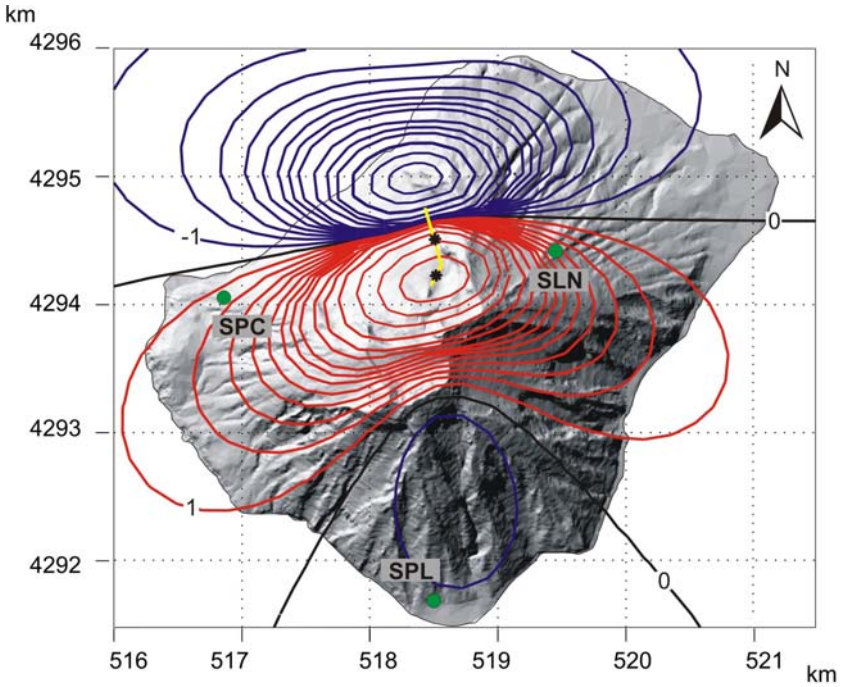

584

585 **Figure 7 –** Piezomagnetic anomaly (contour lines at 1 nT) generated by the intrusive dike. The

586 coordinates are in UTM projection, zone 33 N.

587

588

589

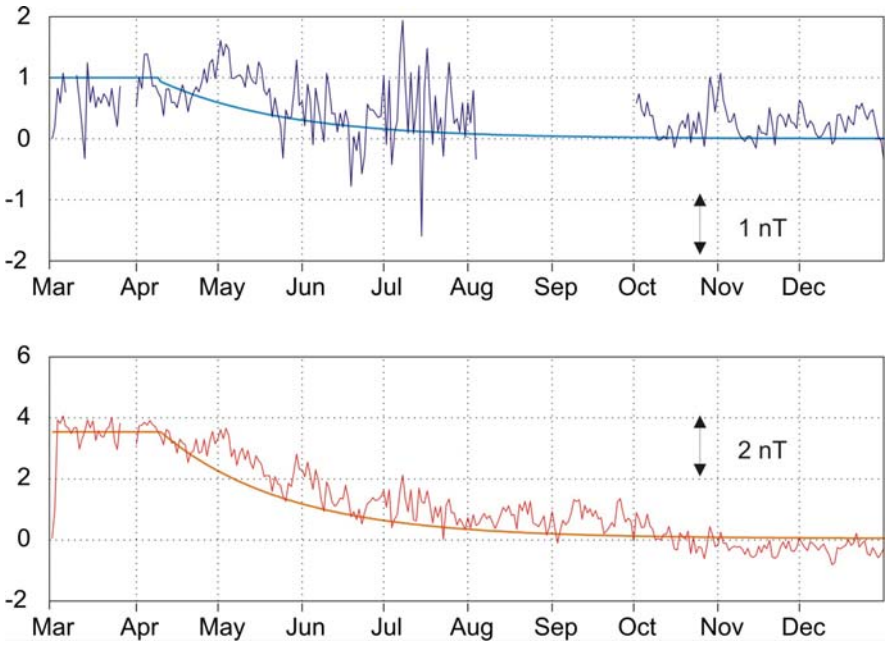

590

591

592 **Figure 8 –** Daily mean variations of the total magnetic field at SPC (blue) and SLN (red) stations

593 referred to CSR. The computed viscoelastic responses at SLN (orange) and SPC (cyan) well match the

594 observations.